3rd International Symposium on Two-Phase Flow Modeling and Experimentation
Pisa, 22-24 September 2004

VIBRATION-INDUCED TWO-PHASE COOLING TECHNOLOGIES FOR HIGH POWER THERMAL MANAGEMENT

S. Heffington, A.Glezer, S. Tillery, and M. Smith
George W. Woodruff School of Mechanical Engineering
Georgia Institute of Technology
Atlanta, GA 30332-0405
Phone: (404) 385 2142
Email: sam.heffington@me.gatech.edu

ABSTRACT

Two technologies for cooling of high-heat flux microelectronics based on enhanced phase-change are described. The first technology is based on a submerged vibration-induced bubble ejection process in which small vapor bubbles that form on and are attached to a submerged heated solid surface are dislodged and propelled into the cooler bulk liquid. This ejection technique involves forced removal of the attached vapor bubbles using a submerged turbulent surface jet generated by a vibrating piezoelectric diaphragm operating at resonance. A small-scale vibration-induced bubble ejection module that produces a submerged liquid jet directed to a boiling heated surface was constructed. Initial test data described in this study include the operating characteristics of the jet as well as its cooling capabilities. The efficacy of this cooling approach is demonstrated using a thermal test die which normally dissipates 83 W/cm^2 at 120ºC in the absence of the jet. When the jet is active, the heat dissipation increases to 220 W/cm^2 (i.e., improvement of 165%) at the same surface temperature.

The second technology consists of a gravity-independent, two-phase closed heat transfer cell, in which heat is removed from the hot surface by the evaporation of a thin liquid film that is produced by the impact of self-propelled atomized droplets. Surface atomization is achieved within the sealed heat transfer cell using a vibration-induced droplet atomization (VIDA) process. The present paper describes the operation of a small-scale VIDA heat transfer cell for cooling desktop microprocessors with particular emphasis on its operating characteristics and cooling capabilities. The effects of internal flow regulation and of geometry and surface characteristics of the heated surface on the cell performance are investigated. Heat fluxes as high as 420 W/cm^2 have been dissipated at die temperatures below 135ºC.

INTRODUCTION

In the microelectronics industry, advances in technology have brought about an increase in transistor density and faster electronic chips. As electronic packages increase in speed and capability, the heat flux that must be dissipated has also increased. Cooling fluxes are projected to reach the 1000 W/cm^2 level for some high power electronic applications [1].

Two-phase heat transfer, involving the evaporation of a liquid in a hot region and the condensation of the resulting vapor in a cooler region, can provide the large heat flux dissipation needed for microelectronic packages to operate at acceptable temperature levels. By changing the phase of the working fluid, a two-phase heat transfer cooling scheme supports high heat transfer rates across moderately small temperature differences. Heat pipes and thermosyphons are examples of efficient heat transfer devices that exploit the benefits of two-phase heat transfer [2-4]. Immersion cooling, which involves the pool boiling of a working fluid on a heated surface, is another example of a two-phase cooling technology used in microelectronic applications [5].

Direct liquid immersion cooling is a highly effective cooling strategy for two reasons: 1) the liquid to vapor phase change greatly increases the heat flux dissipated from the heated surface, and 2) the high thermal conductivity of the liquid medium, compared to that of air, enhances the accompanying natural or forced convection. Previously viewed as incompatible with microelectronic packages, interest in liquid immersion coolers has increased recently because of the need for effective cooling in microelectronic devices (see the review by Bar-Cohen, 1993) [6]. The performance of an immersion cooler at the high heat fluxes required of applications both today and in the future is possible because of the nucleate boiling that occurs with direct contact between the liquid and the hot electronic package. Boiling heat transfer has been widely studied for the last fifty years and has been reviewed by many authors, e.g., Dhir (1998) [7]. A key reason for the efficient heat transfer that occurs during boiling is that buoyancy forces (i.e., gravity) remove the vapor bubbles generated at the heated surface. When the heat flux from the surface is increased past a critical level, a large, possibly catastrophic increase in temperature occurs. This critical heat flux marks the transition from nucleate boiling to film boiling. In film boiling, a thin insulating layer of vapor completely covers the heated surface, which then produces the large temperature increase. This transition occurs at much lower heat fluxes in microgravity environments because buoyancy forces are greatly reduced. Thus, the performance of immersion cooling in these environments is drastically decreased.

A cooling module based on the submerged vibration-induced bubble ejection (VIBE) process in which small vapor bubbles attached to a solid surface are dislodged and propelled into the cooler bulk liquid is a new technology that capitalizes on the benefits of two-phase cooling while improving on traditional pool boiling heat transfer. The VIBE module has a potential in performance to exceed conventional immersion cooling devices because it delays the onset of the critical heat flux. By forcibly removing the attached vapor bubbles with a submerged turbulent jet, the VIBE module dissipates more energy for a given surface temperature than other immersion coolers.

A schematic of one type of VIBE module is shown in Figure 1. The cell has a vibrating driver operating at resonance that generates a round turbulent water jet directed to the immersed microelectronic component. The jet removes the vapor bubbles on the chip surface allowing cooler bulk fluid to wet the boiling surface. The ejected vapor bubbles are cooled and condensed by the bulk liquid. The pool of liquid is cooled by chilled water circulating through a copper condenser coil mounted in the cell. The entire cell can be made very small, and the driver requires only a few watts of energy to operate.

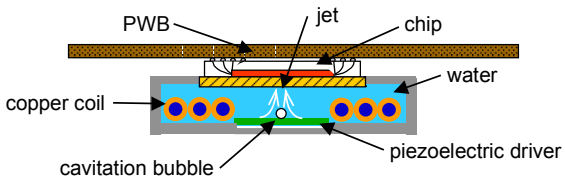

Figure 1. *Schematic of a VIBE heat transfer module.*

A cooling module based on the VIDA principle is another new technology that capitalizes on the benefits of two-phase cooling while improving on heat pipe performance by eliminating the wicking structure and employing an active means to transport the liquid phase to the heat source [8,9]. Because of the absence of the wick structure the performance of a VIDA cell is not limited by the liquid transfer capacity to the boiler section. Furthermore, the VIDA cell also has the potential in performance to exceed conventional thermosyphons because it utilizes thin film evaporation in the evaporator section and therefore can minimize temperature gradients that cause thermal stresses. The evaporation of a thin film prevents the formation of an insulating vapor blanket that can exist in pool boiling situations. Also, the momentum of the atomized droplets is sufficient to propel them through the vapor layer and to spread the impinging liquid into a thin film on the heated surface. While the VIDA cell has clear advantages over conventional heat pipes and thermosyphons due to the production of a thin evaporating film, in common with thermosyphons, the previous configurations were gravity driven and must be operated in a nearly horizontal orientation [10].

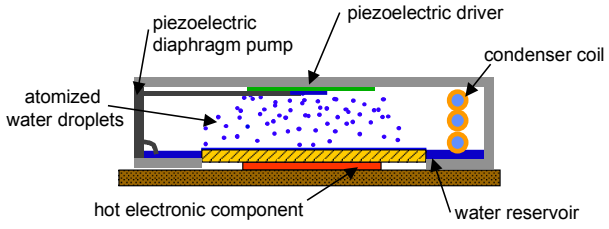

Figure 2. *Schematic of orientation-independent VIDA heat transfer cell*

A schematic of one type of VIDA cell is shown in Figure 2. The cell has a vibrating driver that creates a shower of small diameter secondary droplets by breaking up larger primary drops that form on the driver. The secondary droplets are propelled toward the heated surface where they form a thin film of liquid. This liquid film evaporates, and vapor fills the interior cavity of the cell. Chilled water is circulated through a copper condenser coil mounted in the cell. The vapor condenses on the surface of the copper coil, and the condensed liquid is then returned via a piezoelectric diaphragm pump to the driver where it again is atomized and the process is repeated. The entire cell can be made very small and the driver requires only milliwatts of energy to operate.

The liquid-cooled cell shown in Figure 2 is primarily designed for controlled thermal management of microprocessors during the burn-in process [11,12]. Several VIDA heat transfer cells that use forced air convection as the global cooling method have been constructed and tested [13-16]. These air-cooled cells use a fin array and fan (instead of circulating chilled water) for global cooling of the cell condenser. Heat fluxes over 100 W/cm^2 are dissipated while keeping the heater temperature below 100ºC while using standard cooling fans. These VIDA heat transfer cells have used both water and FC-72 as the working fluid, and they have proven more effective than solid metallic conductors of equal volume [16]. This paper details the results of a new orientation-independent atomization process in which the droplets striking the heater surface are accelerated with a synthetic jet. Current plans are underway to incorporate this new atomizer into a VIDA cell as shown in Figure 2. By using an orientation-independent design, the VIDA cell be applicable to high-heat flux applications on earth and in space such as radar cooling, laser heat dissipation, and microelectronic thermal management of moving systems.

THE VIBE JET

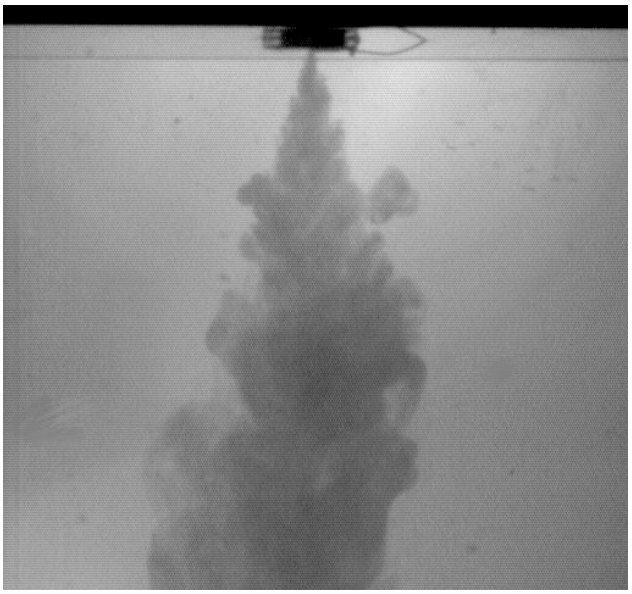

Figure 3. *Dye visualization photograph of the VIBE turbulent jet. The dye is entrained radially from an injection port near the edge of the diaphragm.*

The key technology in the VIBE cell is the submerged turbulent water jet. This jet is produced by an actuator comprised of a vibrating circular diaphragm mounted to a fixed surface. A flow visualization photograph of the jet is shown in Figure 3. The jet is visualized by a streak of dye that is entrained radially from an injection port near the edge of the diaphragm above the jet. The photograph was made using a Kodak Motion Corder SR-Ultra high-speed camera. As proposed by Glezer et. al. [17], the diaphragm-driven turbulent water jet has finite linear streamwise momentum, but in contrast to conventional jets, it is formed without net mass injection across the flow boundary and is

comprised entirely of axisymmetrically entrained fluid. After the oscillating frequency of the diaphragm surpasses a given threshold, the jet appears near the center of the diaphragm along with a small cluster of cavitation bubbles. Pressure oscillations due to vortex ring coalescence in the liquid near the surface of the diaphragm result in the time-periodic formation and collapse of these cavitation bubbles, which entrains surrounding liquid and generates the turbulent jet directed normal to the surface of the diaphragm and flowing away from its center. Even though the jet results from time-periodic excitation, the time-averaged jet structure is similar to that of a conventional turbulent round jet. The jet width and centerline velocity are both linear functions of the distance from the diaphragm. In the present investigation, the formation characteristics and the heat transfer capabilities of the jet are described.

The jet flows normal to the surface of the submerged actuator comprised of a 0.39-mm-thick circular brass diaphragm having a diameter of 18.2 mm driven by a concentrically mounted 0.19-mm-thick piezoceramic wafer having a diameter of 11.6 mm. The diaphragm was glued concentrically over a cylindrical chamber with a diameter of 15 mm and a 13 mm depth contained within an acrylic cube measuring 25 mm x 25 mm x 19 mm. The cube was fitted with a 3.2 mm x 10-32 nylon elbow such that the mounting chamber could be provided with air via an air tube as depicted in Figure 3. The glue used was an 8:1 weight mixture of Stycast 2651 and Catalyst 11, both from Emerson & Cuming. The actuator was driven at the resonance frequency of its first axisymmetric mode of vibration (nominally 7 kHz) using a laboratory function generator and a high voltage (max. 120 V_{rms}) broadband (25 Hz–150 kHz) amplifier. In order to adjust the distance between the actuator and the heated surface, the acrylic cube was bolted to two aluminum shims each measuring 30.5 mm x 6.3 mm x 25.4 mm. Each of these shims contained six adjustment holes at 3.8 mm increments along their respective vertical centerlines.

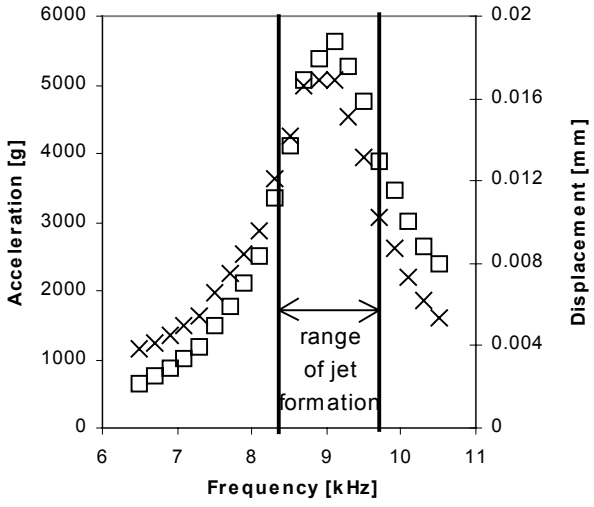

Figure 4. *Driver acceleration (□) and displacement (x) as a function of frequency.*

The driver acceleration and displacement are plotted as a function of frequency in Figure 4. The actuator displacement at the center of the piezoelectric diaphragm was measured using a laser vibrometer. While the driver was submerged and energized, the laser was directed to the point of maximum amplitude on the piezoelectric wafer located on the dry side of the actuator. The acceleration was calculated from the measured displacement data. A jet formed above a threshold acceleration of 3300 g and threshold displacement of 0.012 mm.

VIBE HEAT TRANSFER MODULE

Understanding the required conditions to produce a jet is crucial to the development of the VIBE heat transfer module. Insufficient driver acceleration or displacement would allow vapor to insulate the chip leading to catastrophic dry out. Operating above the measured threshold acceleration and displacement shown in Figure 4 ensures continual operation of the jet. In order to test the cooling efficacy of the VIBE jet, an immersion VIBE heat transfer module was constructed. The experimental set-up was open to the atmosphere and no effort was made to condense or collect the evaporated liquid.

Each experiment was conducted in a small circular water tank with an inner diameter of 13 cm and a height of 4 cm. In the bottom of the tank, a thermal test die was mounted with its heated surface exposed to the liquid pool. In order to take more precise measurements, the heat-spreader lid was removed from the die thus exposing the 1.18 cm^2 silicon chip beneath. The output of the imbedded temperature sensors within the test die was measured, displayed, and recorded with a Fluke NetDAQ data acquisition system. The power supplied to the test die for heating was provided by a 900 W Sorensen DCR 150-6B power supply. To test the heat transfer potential of the jet, the aforementioned actuator and shim assembly was placed within the water tank with the center of the diaphragm aligned to the center of the thermal test die as depicted in Figure 5. In each of the experiments, the water tank was filled with distilled water such that both the diaphragm and the test die were both submerged.

Photographs of an operational jet removing vapor bubbles from the test die using the set-up described above are presented in Figure 5. The photographs are taken 0.02 s apart after the piezoelectric disk is energized from rest. These images indicate the ability of the jet to rapidly force vapor bubbles of various diameters from the die surface into the bulk liquid where they condense. The jet forces the vapor bubbles to coalesce and then the turbulent flow of the jet forces the larger bubbles away from the surface of the die.

VIBE HEAT TRANSFER RESULTS

The procedure for the VIBE heat transfer experiments was as follows. The actuator was placed in the desired location relative to the thermal test die. The liquid reservoir was filled with distilled water, and then the driver was energized. After the jet formed the thermal test die was powered on. The power dissipated by the die was measured by monitoring the steady-state voltage and current levels applied to the die. The heat flux removed from the die surface was estimated by dividing the total power dissipation by the area of the die (1.18 cm^2). The temperature of the chip surface was measured using the embedded temperature sensors. In each test, the test die was powered up in 5 V

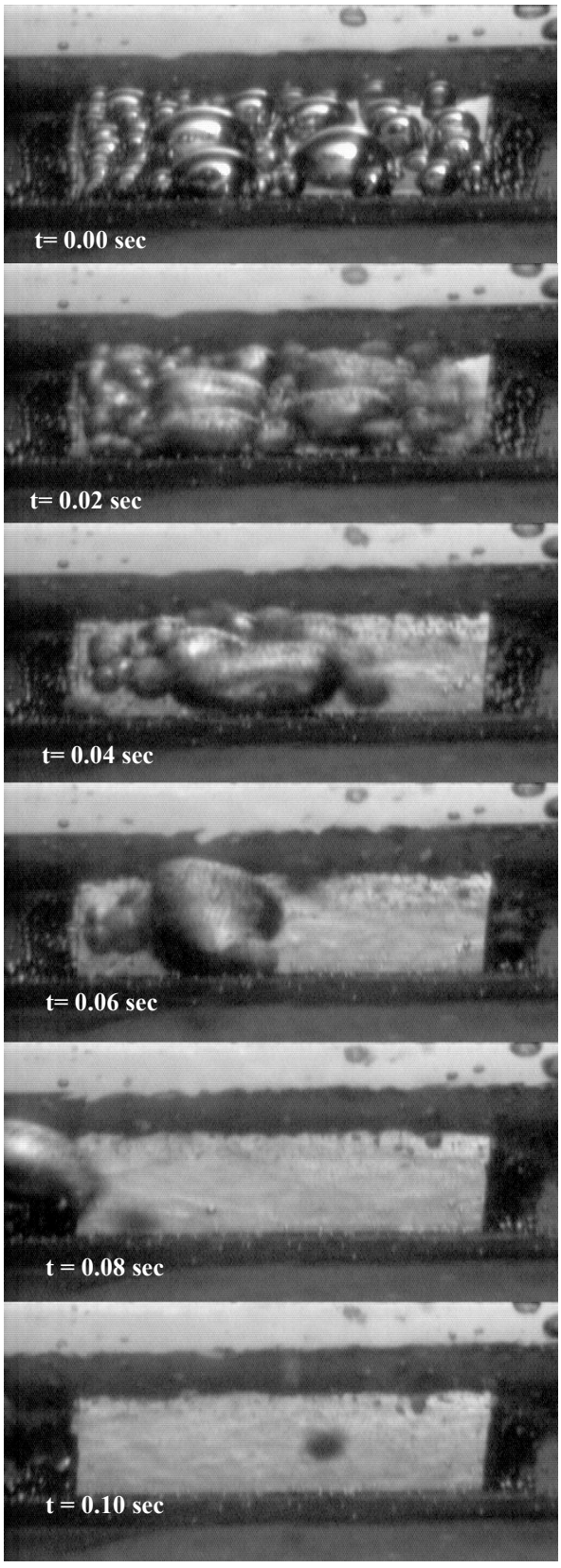

Figure 5. *Photographs of vibration induced bubble ejection.*

increments, and for each increment, the surface temperature was allowed to reach steady state before it was recorded. The test was terminated when the temperature of the test die was 115°C, 5°C lower than the maximum allowable value of 120°C. For those cases in which the jet was on, the diaphragm was driven in its first mode of vibration with approximately 90 V_{rms}.

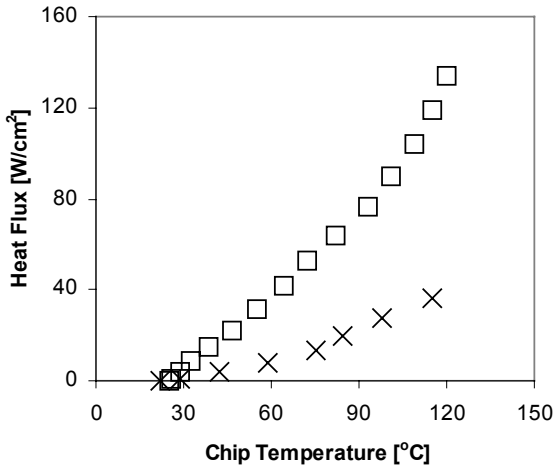

Figure 6. *The heat flux from the thermal test die with the jet on (□) and with the jet off (x).*

In the first experiment, the effect of the jet impinging directly on the thermal test die was measured. Data was obtained for two different scenarios: pool boiling with the jet on and pool boiling with the jet off. The results are shown in Figure 6. Below a chip temperature of 100ºC (the onset of boiling) the presence of the jet increased the amount of heat dissipated for a given temperature. The turbulent jet provided forced convection heat transfer from the chip to the pool of water. The added turbulent mixing and bulk motion present when the jet was on compared to the free convection heat transfer when the jet was off resulted in higher heat fluxes. Above 100ºC, the VIBE effect was present when the jet was on. By removing the insulating vapor bubbles from the surface of the die, the heat flux dissipated as a function of die temperature increased at a faster rate. At a die temperature of 115ºC, the heat flux dissipated increased from 36 W/cm^2 with the jet off to 119 W/cm^2 when the jet was on. This 230% improvement was a result of the VIBE jet increasing the overall heat transfer coefficient through increased convection and the removal of insulating vapor bubbles.

As mentioned earlier, each of the shims that supported the actuator had six equally spaced holes that were used to set the separation distance between the diaphragm and the surface of the thermal test die. At separation distances larger than 10 mm, the jet momentum was not sufficient to remove all the vapor bubbles. The remaining bubbles caused the decrease in the heat flux from the die. The ability of the VIBE module to dissipate over 110 W/cm^2 of heat flux at a die temperature of 103ºC with a driver to die separation distance of only 1.9 mm indicates that a small-scale VIBE module could be produced for microelectronic thermal management.

The final set of experiments for pool prototype examined the effect of the impingement angle of the jet. The actuator was set at the optimum vertical separation distance by bolting it to the appropriate holes on the shims. The impingement angle was set by rotating the actuator to the appropriate angle using the bolts as the point of rotation. For each angle, the placement of the center of the actuator with respect to the thermal test die was altered as to maintain a constant distance between the two surfaces. This measured data shows that the impingement angle had little effect on the heat flux, particularly above a die temperature of 100ºC. For all of these impingement angles, the jet still removed the vapor bubbles that formed on the die. Thus, the die experienced almost the same thermal conditions for each impingement angle resulting in nearly identical heat transfer results. This ability to vary the impingement angle of the jet with little loss in performance provides further design flexibility in the implementation of a VIBE heat transfer module for microelectronic cooling applications.

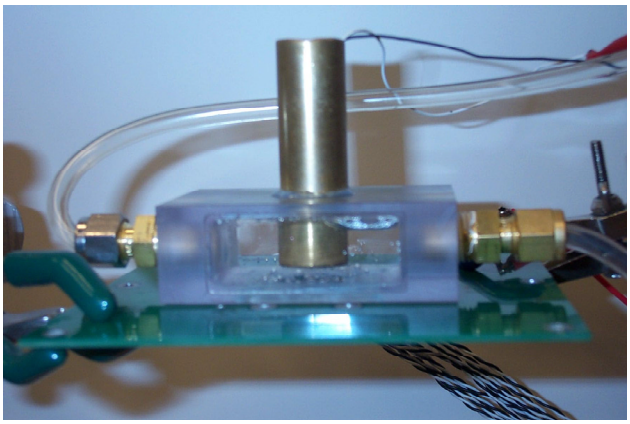

Figure 7. *The flow-through VIBE cell.*

A photograph of another VIBE heat transfer cell is shown in Figure 7. This cell has an inlet and outlet to allow for a flow of liquid removing the heat dissipated by the thermal test vehicle. The module was machined from a solid block of Lexan measuring 51 mm wide x 25 mm high x 76 mm long. The internal dimensions of the module are 46 mm wide x 18 mm high x 48 mm long. In order to control the bath temperature within the module, a crossflow was instigated within the cell. This was done by tapping either end of the cell such that a 1/4 NPT fitting could be screwed into each tapped hole. Using these fittings, subcooled water was supplied to the cell from a chilled water bath. This was done in such a way as to allow for the water temperature as well as the flow rate into the cell to be varied.

The piezoelectric diaphragm glued to the hollow brass rod was inserted into a 19 mm diameter hole drilled into the top of the cell. The diaphragm was lowered into the cell until its surface was approximately 5.7 mm from the heated surface since this is the distance for optimal heat transfer enhancement resulting from direct impingement by the jet [18].

After mounting the VIBE heat transfer module to the board onto which the test die was fixed, the hoses were connected to the cell to allow for water from the water bath to flow through the cell. Once the cell was filled with water and all air bubbles were removed from the cell, the driver was energized. After the jet formed, the thermal test die was powered on. The power dissipated by the die was measured by monitoring the steady-state voltage and current levels applied to the die. The heat flux removed from the die surface was estimated by dividing the total power dissipation by the surface area of the die (1.18 cm^2). The temperature of the chip's surface was measured using the temperature sensors embedded within the chip. In each test, the test die was powered up in 5 V increments, and for each increment, the surface temperature was allowed to reach steady state before it was recorded. The test was terminated when the temperature of the test die was 115°C, 5°C lower than the maximum allowable value of 120°C. For those cases in which the jet was on, the diaphragm was driven in its first mode of vibration with approximately 90 V_{rms}.

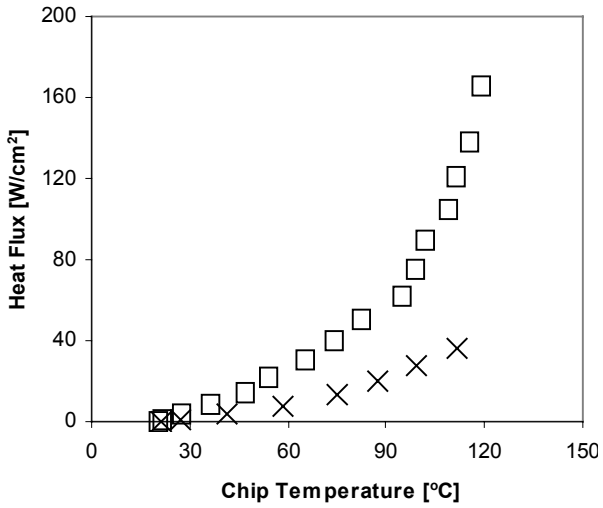

Figure 8. *The heat flux from the thermal test die with the jet on (□) and with the jet off (x).*

In the first experiment, the water bath was set such that the water it provided to the heat transfer cell remained at a constant 20°C, and the flowrate of the water bath was set such that the water flowed at a rate of 15 mm/s through the cell. Data was collected for two different scenarios: channel boiling with the jet on and channel boiling with the jet off. The results of this experimentation can be seen in Figure 8. Without the jet actuated, the crossflow within the cell did little to remove the insulating vapor bubbles from the surface of the test die. Without the jet actuated, the heat flux from the die to the water was 36 W/cm^2 at a surface temperature of 111°C. With the jet actuated, the heat transfer was much more significant. Below a chip temperature of 100°C (the onset of boiling) the presence of the jet increased the amount of heat dissipated for a given temperature. The turbulent jet provided additional forced convection heat transfer from the chip to the flowing water within the cell. The added turbulent mixing and bulk motion present when the jet was on compared to the very mild amounts of forced convection heat transfer when the jet was off resulted in higher heat fluxes. Above 100°C, the synthetic jet removed

the insulating vapor bubbles from the surface of the die. As a result of this, the heat flux dissipated as a function of die temperature increased at a faster rate. While the crossflow alone had little effect on the heat dissipated from the surface, the flow, coupled with the synthetic jet, worked well to sweep the newly discharged bubbles downstream where they were allowed to condense. In addition to this, the crossflow provided cooler water to the jet thus allowing for more heat transfer due to the forced convection by the jet on the heated surface. At a die temperature of 111°C, the direct impingement of the jet onto the heated surface increased the heat flux from the surface by 236% to a value of 121 W/cm^2. This improvement was a result of the synthetic jet increasing the overall heat transfer coefficient through increased convection and the removal of the insulating vapor bubbles.

In the second experiment, the water bath was again set such that the velocity of the water traveling through the cell was approximately 15 mm/s, but in this experiment, the temperature of the water provided by the water bath was varied from 20°C to 60°C. The results of this experimentation can be seen in Figure 9. As was previously described, impingement by the synthetic jet increased the amount of heat dissipated from the thermal test die by 236% for a die temperature of 111°C. When the temperature of the water in the bath was increased to 60°C, direct impingement by the jet increased the amount of heat dissipated by the surface by approximately 300%. This increase in the overall heat transfer improvement provided by the synthetic jet is attributed to the fact that the strength of the jet remains virtually constant at various bath temperatures. Since the amount of heat dissipated during standard pool boiling decreases as the temperature of the water in the bath increases, the jet provided a greater overall improvement in heat transfer for the higher bath temperature.

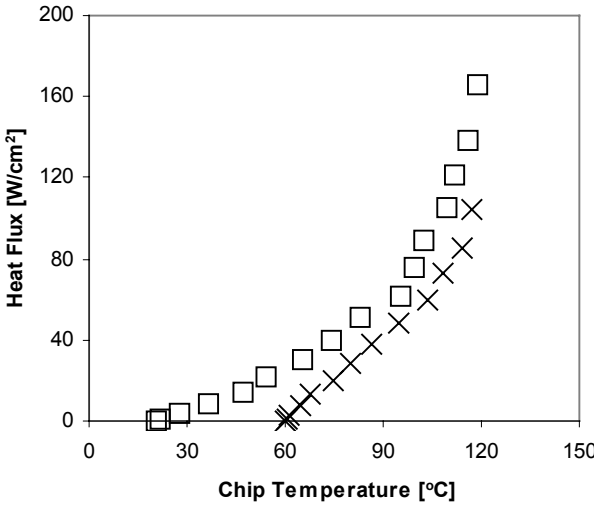

Figure 9. *The heat flux from the thermal test die with the jet on and inlet water temperature of 20°C (□) and with the jet on and inlet water temperature of 60°C (x).*

THE VIDA PROCESS

The VIDA atomizer is comprised of a metallic disc that is bonded on its back surface to a piezoelectric driver. The disk assembly is covered by a continuous thin liquid film supplied by a piezoelectric diaphragm pump. When driven at sufficient resonance acceleration levels, the atomizer generates secondary droplets by bursting the primary liquid layer. The secondary droplets are propelled away from the vibrating surface and can be transported towards and impact upon a remote heated surface. The frequency and amplitude of the driving signal are important parameters that must be properly controlled in order to achieve the liquid break-up in the VIDA process.

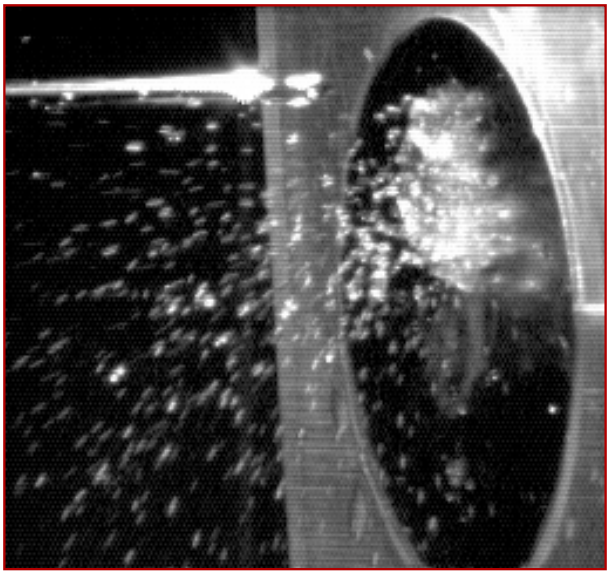

Figure 10a. *Ejected secondary droplets with the atomizer in a vertical orientation. The supply tube is normal to the atomizer.*

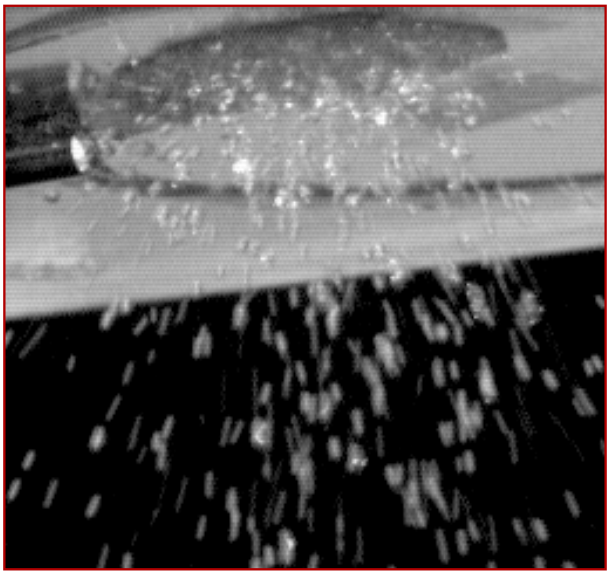

Figure 10b. *Ejected secondary droplets with the atomizer in a downward-facing horizontal orientation. The supply tube is tangential to the atomizer.*

In the present work a 31 mm diameter piezoelectric atomizer is glued to a plastic holder. Liquid is supplied to the atomizer by pumping liquid through a stainless steel tube having an outer diameter of 1.9 mm and an inner diameter of 1.15 mm. The flow rate supplied by the piezoelectric diaphragm pump can be varied from 0.7 to 7.56 mL/min. As shown in the photographs in Figures 10a and 10b, the orientation and proximity of the supply tube is flexible. As long as the liquid ejected from the tube contacts the atomizing diaphragm, a spray of droplets will result. The vibration of the atomizing piezoelectric disk forces the liquid droplets from the supply tube to wet the surface of atomizer. The resulting thin liquid layer is accelerated by the motion of the driver and results in atomization of the liquid into secondary droplets that are uniform in size. The size and speed of the secondary droplets is a function of the excitation frequency and amplitude of the atomizer.

VIDA HEAT TRANSFER

While earlier versions of VIDA cells were based on an air-side fan and fin array [13-16] or liquid-cooled condenser coil [11,12], the present configuration is designed for thermal assessment of the new orientation-independent VIDA atomizer. The atomizer produces a liquid spray used to cool a thermal test vehicle. The experimental set-up was open to the atmosphere and no effort was made to condense or collect the evaporated liquid.

A schematic of the orientation-independent VIDA heat transfer assessment experiment is shown in Figure 11. The set-up consists of a 25 mm diameter atomization piezoelectric disk, a piezoelectric diaphragm pump, and a thermal test vehicle. The atomization disk is mounted to a plastic holder using RTV sealant and oriented vertically. The 25 mm square piezoelectric diaphragm pump, located a short distance from the atomizer, continually supplies room temperature water from a reservoir to the atomizer. The thermal test vehicle consists of several resistive heater elements covered by an integrated copper heat spreader. Thermocouples are mounted in the heat spreader to measure the evaporation surface temperature. This assessment set-up allows for several parameters to be varied including the angle of heater, the distance between the heater and the atomizer, the liquid flow rate out of the pump, and excitation voltage of the atomizer.

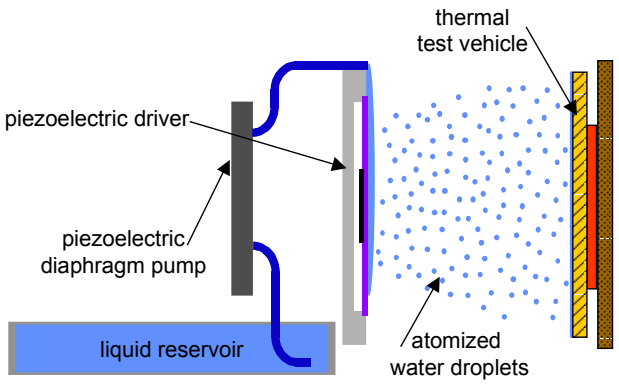

Figure 11. *Schematic drawing of a VIDA heat transfer experiment designed for assessment of an orientation-independent atomizer*

VIDA HEAT TRANSFER RESULTS

The VIDA orientation-independent atomizer is tested using a packaged Intel thermal test vehicle in which the die area is 1.18 cm^2 and the area of the integrated heat spreader is 9.61 cm^2. The thermal test vehicle is placed in the desired location relative to the atomizer and pump (Figure 11). The liquid reservoir is filled with water, the pump is activated, and the atomizer is energized. After the liquid spray is initiated, the die is powered. The power dissipated by the water spray contacting the thermal test vehicle is measured by monitoring the steady-state voltage and current levels applied to the thermal package. The heat flux removed from the thermal test vehicle is estimated by dividing the power dissipation level by the area of the die (1.18 cm^2). The temperature of the lid of the thermal test vehicle (the evaporation surface) is measured using thermocouple sensors.

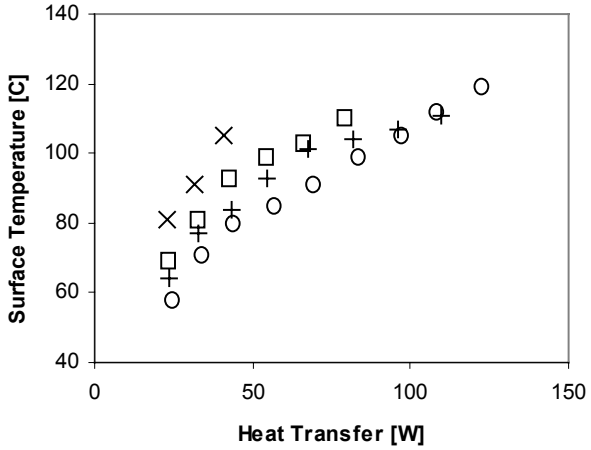

Figure 12. *Effect of separation distance between atomizer and thermal test vehicle. Separation distance = 0.5 cm(×), 1.25 cm (□), 2.0 cm (+), and 4.5 cm (○).*

In the first experiment, the VIDA spray impacted directly on the vertically oriented thermal test vehicle as shown in Figure 11. The heat transfer from the test vehicle was measured as a function of surface temperature for four different separation distances between the atomizer and the thermal test vehicle. In these experiments, the excitation voltage of the atomizer was a constant 21 V_{rms} and the pump flow rate was a constant 7.56 mL/min. The results in Figure 12 show the effect of distance between the heater and atomizer when the two devices are maintained at a constant elevation. These results show that the temperature of the evaporating surface decreases for a given heat transfer level as the separation distance increases. As the separation distance decreases, the area of the thermal test vehicle covered by atomized droplets decreases. Also, the quantity of atomized droplets entrained in the vapor flow leaving the heated surface increases as the separation distance decreases. The excitation frequency of the atomizer is approximately 3.3 kHz. At this frequency, the secondary droplets are 220 microns in diameter, a size that is easily entrained in a flow of steam. High-speed camera images of the evaporation process indicate that significant numbers of secondary droplets are captured by the vapor flowing upward from the heated surface. The increased entrainment of ejected droplets combined with the decrease in spray coverage area results in a higher temperatures for a given heat transfer level as the separation distance decreases. The present atomization set-up is capable of dissipating 120 W while maintaining the

evaporation surface below 125ºC, which is an improvement over previous VIDA cells operating at atmospheric pressures.

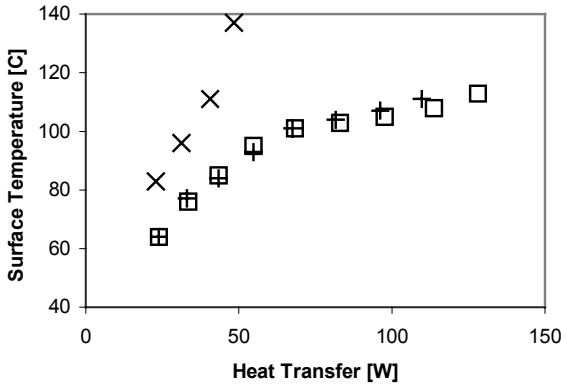

Figure 13. *Effect of diaphragm pump flow rate. Flow rate = 0.702 mL/min (×), 3.43 mL/min (□), and 7.56 mL/min (+)*

The effect of the volume flow rate of water through the piezoelectric diaphragm pump on the surface temperature and heat transfer rate from the die is investigated while maintaining the separation distance between the die and atomizer fixed at 2.0 cm. In Figure 13, the water flow rate is set at 0.7, 3.43, and 7.56 mL/min (excitation voltage is maintained at $21V_{rms}$ and the set-up is shown in Figure 11). The results indicate identical temperature performance when the flow rate is greater than or equal to 3.43 mL/min regardless of heat transfer rate. At both of these pump flow rates, the flow rate of atomized liquid droplets is nearly identical. Visualization indicates that at the higher flow rate the atomizer is not capable of ejecting all the liquid from the pump, and some of the water rolls down the disk without being atomized. Thus, the thermal test vehicle sees nearly identical sprays for both of the higher flow rate conditions. However, at the slowest flow rate of 0.7 mL/min the temperature is significantly higher for a given heat transfer level. At this level of flow rate, the heated surface does not receive enough water causing dry spots to form. Above a heat transfer level of 50 W, the thermal test vehicle suffers complete dry-out and temperature run-away due to the lack of liquid to cool the surface.

The thermal effectiveness of the orientation-independent VIDA spray was also investigated by varying the atomization driver voltage level. The separation distance was held constant at 4.5 cm, while the flow rate was also maintained at a constant 7.56 mL/min. As the driver voltage level increases, the energy transferred from the driver to the spray also increases. This added energy increases the velocity and momentum of secondary droplets striking the heated surface. Although the relationship between voltage level and droplet velocity is not linear, an increase in voltage level should result in a decrease in surface temperature for a given heat transfer level. The results indicate this is true, particularly above a heat dissipation level of 100 W. Visual inspection of the droplet spray indicates at the higher voltage levels, the secondary droplets containing more momentum are less effected by gravity and the evaporating liquid. At the higher voltage level, the secondary droplets are better able to wet the heated surface, and fewer droplets are entrained in the vapor leaving the thermal test vehicle. At an evaporation surface temperature of 108ºC, there is a 51% improvement in heat dissipation level by doubling the driver voltage level.

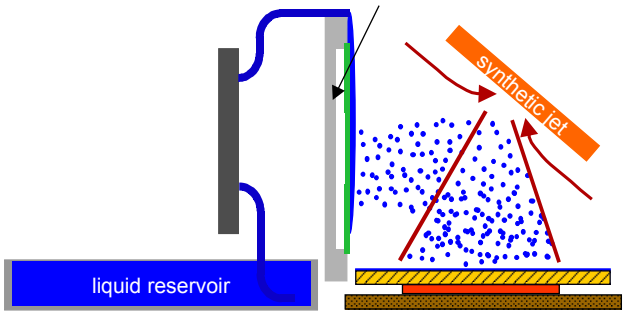

Figure 14. *Schematic drawing of a synthetic jet-VIDA heat transfer experiment*

In an effort to improve the heat flux dissipate capabilities of the VIDA process, a synthetic jet was added to the set-up as shown in Figure 14. This synthetic jet entrains the surrounding air and atomized droplets producing a stream of uniform high speed (up to 90 m/s) droplets travelling toward the heated surface. The added velocity associated with the synthetic jet-VIDA combination enables the droplets to better spread into a thin film on the heated surface compared to the VIDA only process. The extra velocity also helps the droplets avoid entrainment from the resulting vapor flow.

The effect of the synthetic jet-VIDA combination is shown in Figure 15. The heat flux dissipated is plotted as a function of heater surface temperature. This data indicates a significant increase in heat flux dissipation compared to the VIDA only process. The addition of the synthetic jet results in a critical heat flux of 420 W/cm^2 at a surface temperature of 133ºC.

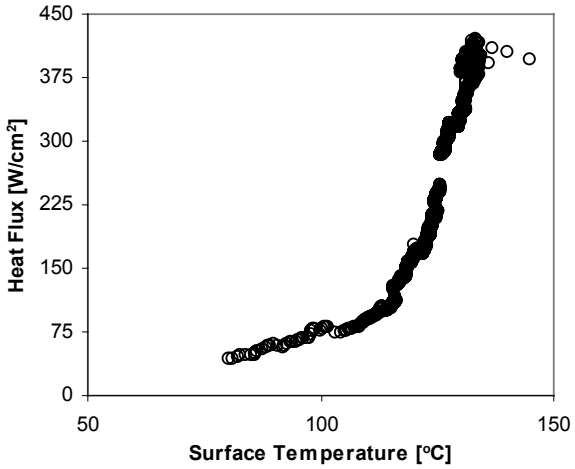

Figure 15. *The heat flux from a thermal test vehicle as function of surface temperature for the synthetic jet-VIDA combination*

CONCLUSIONS

Pool-boiling enhancement heat transfer technology that is based on a new vibration-induced bubble ejection mechanism (VIBE) has been demonstrated. In this technology, a piezoelectric diaphragm is used to produce a submerged round turbulent jet that is directed at a microelectronic package. The jet removes the vapor bubbles that form on the package during nucleate boiling and forced them back into the cooler bulk liquid where they condense.

The present set of experiments used distilled water as the working fluid under atmospheric conditions. The test module generated a water jet with enough momentum to remove vapor bubbles from the surface of a test die. Heat fluxes up to 135 W/cm^2 were achieved in a compact geometry requiring approximately 1 W of input power. This is a heat flux increase of 230% compared to traditional pool boiling with no jet, for the same surface temperature.

The performance of the VIBE process in terms of the heat flux for a given surface temperature increased as the separation distance between the actuator and the surface of the die decreased. The impingement angle of the jet had relatively little effect on the heat flux.

For the flow prototype cell, the jet removed the vapor bubbles that formed on the heater during nucleate boiling and forced them back into the cooler bulk liquid where the crossflow within the cell swept them downstream where they condensed. This test module generated a water jet with enough momentum to remove vapor bubbles from the surface of a test die. Heat fluxes up to 165 W/cm^2 were achieved in a compact geometry requiring approximately 1 W of input power. This is a heat flux increase of 230% compared to traditional channel boiling with no jet, for the same surface temperature. It was also determined that by increasing the temperature of the water flowing through the cell from 20^{o}C to 60^{o}C, the percent improvement in heat dissipation resulting from impingement by the sythetic jet increased to 300%.

These heat transfer results demonstrate the potential of this VIBE process to effectively manage heat removal from high power microelectronics and for the thermal management of microprocessors and other electronic hardware. Future work will focus on incorporating the VIBE jet into a sealed small-scale heat transfer cell in which the internal pressure will be controlled.

A heat transfer technology based on a new orientation-independent droplet atomization mechanism that is suitable for thermal management of microprocessors and other electronic hardware is demonstrated. An atomizer based on vibration induced droplet atomization (VIDA) combined with a piezoelectric diaphragm pump provides a continual flow of small diameter droplets that are propelled toward a heated surface where they form a thin liquid film. The droplets can be sprayed in any direction as long as liquid from the pump encounters the atomizer. The thin liquid film evaporates on the hot surface and the vapor is released to the surroundings. In future cell designs, the atomizer and pump with be an integral part of a closed cell in which the vapor is condensed on an air-cooled surface or a liquid-cooled coil.

The present experiment uses water as the working fluid and heat transfer rates of up to 230 W are achieved in a rather compact geometry requiring less than 1 W of input power. The tests reported here compare the effectiveness of the new orientation-independent VIDA process in atmospheric conditions. The advantage of this configuration over previous designs is the elimination of liquid transport by gravitational forces. As shown, it is possible to atomize a liquid layer into micron-sized droplets in both a downward and vertical orientation.

The present work has also shown that the performance of the VIDA process in terms of the heat flux for a given surface temperature increases as the separation distance between the heater and atomizer increases. Comparative tests using different water flow rates from the pump indicate for a given heat transfer rate the surface temperature decreases as the flow rate increases up to 3.43 mL/min. Any pump flow faster than 3.43 mL/min does not produce an improvement in heat transfer performance because the added flow is not atomized by the driver. For a given surface temperature, the heat dissipation increases by 51% when the atomizer driving voltage is doubled. Finally, the present measurements show the addition of a synthetic jet extends the critical heat flux to 420 W/cm^2 from a surface at 133ºC.

ACKNOWLEDGMENT

This work was supported in part by NASA's Microgravity Program and by DARPA.

REFERENCES

[1] Zerby, M. and M. Kuszewski., Final Report on Next Genreation Thermal Management (NGTM) for Power Electronics, NSWCCD Technical Report TR-82-2002012, March 2002.

[2] Peterson, G. P., *An Introduction to Heat Pipes*, John Wiley & Sons, Inc.,, New York, pp. 285-326 (1994).

[3] Kiewra, E. W., and P. C. Wayner. "A Small Scale Thermosyphon for Immersion Cooling of a Disc Heat Source," *Heat Transfer in Electronic Equipment,* ASME Symposium HTD-Vol. 57, Bar-Cohen, A. (Ed.), American Society of Mechanical Engineers, New York, pp.77-82 (1986).

[4] Mudawar, I., T. A. Incropera, and F. P. Incropera, "Microelectronic Cooling by Fluorocarbon Liquid Films," *Proc. Int. Symposium of Cooling Technology for Electronic Equipment* (1987).

[5] Arik, M. and A. Bar-Cohen, "Immersion Cooling of High Heat Flux Microelectronics with Dielectrid Liquids", 4th Int. Symposium and Exhibition on Advanced Packaging-Materials-Processes-Properties, Atlanta, pp. 229-247 (1998).

[6] Bar-Cohen, A., "Thermal management of electronic components with dielectric liquids," *JSME Int. J. 36*, pp. 1-25, 1993.

[7] Dhir, V.K., "Boiling heat transfer," *Ann. Rev. Fluid Mechanics 30*, pp. 365-401.

[8] James, A.J., B. Vukasinovic, M.K. Smith, and A. Glezer, "Vibration-induced drop atomization and drop bursting," *Journal of Fluid Mechanics* Vol. 476, pp. 1-28 (2003).

[9] James, A.J., M.K. Smith, and A. Glezer, "Vibration-induced drop atomization and the numerical simulation of low-frequency single-droplet ejection," *Journal of Fluid Mechanics*, Vol. 476 pp. 29-62 (2003).

[10] Denney, D. L., W. Z. Black, J. G. Hartley, and A. Glezer, "High Heat Flux Boiling with Monodisperse Water Droplets,"

Process, Enhanced, and Multiphase Heat Transfer, R. M. Manglik and A. D. Krause, eds., Begel House, Inc., New York, pp. 175-182 (1996).

[11] Heffington, S.N., W.Z. Black, and A. Glezer, "Vibration-Induced Droplet Atomization Heat Transfer Cell for High-Heat Flux Applications" *ITHERM 2002 Proceedings*, San Diego, CA (2002).

[12] Heffington, S.N., W.Z. Black, and A. Glezer, "Two-Phase, Spray Cooling Thermal Management using Vibration-Induced Droplet Atomization Heat Transfer Cells" *Proceedings of the 8th THERMINIC Workshop*, Madrid, Spain (2002).

[13] Heffington, S.N., W.Z. Black, and A. Glezer, "Vibration-Induced Droplet Cooling of Microelectronic Components," *ITHERM 2000 Proceedings,* Vol. 2, Las Vegas, NV, pp.328-332 (2000).

[14] Heffington, S.N., W.Z. Black, and A. Glezer, "Vibration-Induced Droplet Atomization Heat Transfer Cell for Microelectronic Thermal Management," *13th European Microelectronics and Packaging Conference & Exhibition,* Strasbourg, France (2001).

[15] Heffington, S.N., W.Z. Black, and A. Glezer, "Vibration-Induced Droplet Atomization Heat Transfer Cell for Cooling of Microelectronic Components," *The Pacific Rim/ASME International Electronic Packaging Technical Conference & Exhibition,* Kauai, Hawaii (2001).

[16] Heffington, S.N., W.Z. Black, and A. Glezer, "Vibration-Induced Droplet Atomization Heat Transfer Cell for High-Heat Flux Dissipation," *Thermal Challenges in Next Generation Electronic Systems (THERMES-2002),* Santa Fe, NM (2002).

[17] Glezer, A., R. D. James, and J. W. Jacobs, "A round turbulent jet produced by an oscillating diaphragm," *Phys. Fluids 8*, pp. 2484-2495, 1996.

[18] Glezer, A., Heffington, S., Smith, M., Tillery, S., *Enhanced Boiling Heat Transfer by Submerged, Vibration Induced Jets*, 9th Therminic Conference, Aix-en-Provence, France, 24-26 September 2003.